Hindawi
Mobile Information Systems
Volume 2022, Article ID 1274563, 14 pages
https://doi.org/10.1155/2022/1274563

Research Article

Application of Mobile Information Technology in High-Intensity Resistance Training System for Cross-Country Skiing

Jianxin Kang[1] **and Peng Zhang**[2]

[1]*Winter Olympic Academy, Harbin Sports University, Harbin 150008, Heilongjiang, China*
[2]*Exchange and Cooperation Department Academy, Harbin Sports University, Harbin 150008, Heilongjiang, China*

Correspondence should be addressed to Peng Zhang; zhangpeng@hrbipe.edu.cn

Received 9 June 2022; Revised 29 July 2022; Accepted 17 August 2022; Published 20 September 2022

Academic Editor: Imran Shafique Ansari

Cross-country skiing is one of the most important competitive events in the Winter Olympics, and it is also the earliest competitive sports event in China's winter snow events. However, due to the influence of factors such as economic development, climatic conditions, and regional resources, cross-country skiing has developed slowly in China and is still in a relatively backward position compared with developed countries such as Europe and the United States. In this paper, the modeling and analysis of the attitude calculation system is proposed, and the attitude recognition technology is applied to the high-intensity resistance training system of cross-country skiing. Several training elements such as special endurance training goals, training content, training methods, and training monitoring are presented. It demonstrates the rationality and feasibility of the high-intensity resistance training system for excellent cross-country skiers in cross-country skiing and arranges the strengthening training of the upper and lower limbs and waist and abdominal muscles of the athletes in a targeted manner. For 6–9 times a week, each endurance training is about 1–4 hours or strength training is about 15–90 minutes. The fastest time for men is 31 minutes 29 seconds 21, which is 1 second 88 higher than that before training, and the average score has improved by 6 seconds 80; the women's fastest time was 24 minutes 06 seconds 21, which was 4 seconds 22 higher than that before training, and the average score increased by 7 seconds 70.

1. Introduction

With the rapid development of the national economy and the continuous improvement of the quality of life of the public, the demand for spirituality also increases. The number of people participating in extreme sports such as skiing and rock climbing is increasing year by year. At the same time, China's successful bid to host the 2021 Winter Olympics and the state's encouragement of "300 million people to participate in the ice and snow sports plan" have brought new vitality and attention to the field of ice and snow sports in China. The number and scale of ski events have continued to expand, and the host cities have also expanded from northern cities to southern cities. At the same time, the demand for the training of skiers is also increasing. Compared with European and American countries, the number of professional ski athletes in China still needs to continue to increase. The cultivation of a professional skiing athlete requires a huge investment of money and energy from the state in every link from selection and training plan to coach training. The degree of completion and completion time of a skier's movements rely solely on the judge's subjective judgment and simple time and equipment records. There is still a certain gap in accurately judging and restoring the skier's movement process. For the skier's training evaluation and competition performance evaluation, it is necessary to propose an effective method and accurate evaluation system method. There is a big gap in the judging standards of each type of competition, but the judging standards are nothing more than two types of skiers' posture and skiing speed. The key to objectively judging the performance of skiers is to restore the posture data and paths of the skiers' movement process. It can accurately detect the change of the skier's posture, provide

data support for the evaluation of the skier's performance, and provide safety guarantee for the skiing process. To realize the transformation from a sports power to a sports power, it is necessary to change the current situation of uneven development of ice and snow sports, give priority to the development of competitive cross-country skiing as a breakthrough for the improvement of snow sports, and promote the improvement of the overall level of cross-country skiing in China.

Intense resistance exercise and subsequent training alter protein turnover in skeletal muscle, but the effect on muscle hypertrophy after resistance exercise training is unknown. The goal of Reidy et al. was to determine whether post-absorptive muscle protein turnover after 12 weeks of resistance exercise training (RET) plays a role in muscle hypertrophy, identifying the underlying molecular mechanisms responsible for altered muscle protein turnover after training [1]. Research is needed on load control methods and staging descriptions for futsal teams. The purpose of the Freitas study was to report and analyze internal training loads in futsal macrocycles, using the Session Rating of Perceived Movement (Session-RPE) method, calculated total weekly training load, monotonicity, and stress over 37 weeks [2]. Patients who are unable to perform traditional resistance training may benefit from this technique by increasing local muscle mass, strength, and endurance when exercising with lower resistance. The purpose of the Miller et al. study was to systematically evaluate the systemic effects of blood flow restriction training combined with exercise intervention, and it is unclear what effects BFR may have on other body systems, such as the cardiovascular and pulmonary systems [3]. The effect of local vibration on muscle hypertrophy during resistance exercise. The purpose of the Drummond et al. study was to determine the effect of local vibration on muscle hypertrophy. The results of the study showed that the application of local vibration need not be included in the RT program of untrained individuals [4]. Maleev et al. aimed to assess the body reserve of skiers developing local area muscular endurance (LRME), static exercise, and resistance to hypoxia and described a regression model comparing key indicators of morphofunctional and metabolic status in athletes [5]. Dias et al. study focused on reviewing the interaction between immunological parameters and overtraining syndrome, and the correlations between exercise, immune system, and susceptibility to URTIs were assessed primarily in individual and endurance exercise [6].

Combining computer vision with motion will have great practical value. Zhu proposed a motion assistance evaluation system for human posture recognition based on deep learning algorithm. When the traditional motion assistance system is introduced into sports training, the motion process can be monitored through sensors and other equipment, the training information of athletes can be obtained, and the athletes can be assisted in their technical actions. A retrospective analysis was performed [7]. However, traditional systems must be equipped with multiple sensor devices, and the motion information provided must be accurate. Babu and Heath study aimed to explore the potential of mobility assistive technology (MAT) as a career tool for blind workers (BW), using fitting theory to analyze observational and interview data from organizations familiar with hiring, training, and recommending BW [8]. Cross-country squatting performance is primarily determined by the forces generated during the piling phase, enhanced by trunk flexion and extension movements. Rosso et al. study, which aimed to validate simulated polarizing action on an adjusted dynamometer and cluster analysis to group participants according to their different impairments, showed good accuracy, sensitivity, and precision [9]. Joint flexion increases and decreases joint loads especially at the knee joint, and the data collected by Kurpiers et al. was used as input to a musculoskeletal model to estimate joint kinematics and joint moments and contact forces of the ankle and knee joints [10]. Based on input data from kinematic and dynamometric analysis, as well as anthropometric data of the monitored person, Bittner et al. can estimate the final momentum of the forces acting on the major joints of the lower body [11]. Sun et al. studied the transition zone contour (cubic function). The research on the athlete's strength state helps to make the body shape better meet the requirements of the competition, and the dynamic differential equation of the athlete is obtained by considering air resistance and ski friction [12].

2. Application Method of Mobile Information Technology in Cross-Country Skiing Resistance Training

2.1. Combination of Cross-Country Skiing Resistance Training and Mobile Information Technology. With the rapid development of computer information technology, the research on human body posture has attracted more and more attention, attracting many universities and research institutions to invest a lot of resources in research, and its applications are also expanding, such as in medicine. Somatosensory games, intelligent sports, and film and television creations have been widely used and have produced great value in use. To meet the requirements of the development of the emerging era, sports methods must be combined with the modern level of science and technology to break the original mode of teaching by words and deeds. The elements of science and technology are better integrated in physical training [13]. The result of the fusion of modern sports and mobile information technology is shown in Figure 1.

As shown in Figure 1, the application of science and technology to sports is the development direction of sports in the future, and it is also in line with the development concept of contemporary society. The rational application of the innovative thinking of "technology + sports" will truly realize the deep integration of science and technology with sports [14]. In today's society, we can already see a lot of intelligent sports equipment and training equipment. In the near future, there will be more and more intelligent sports equipment.

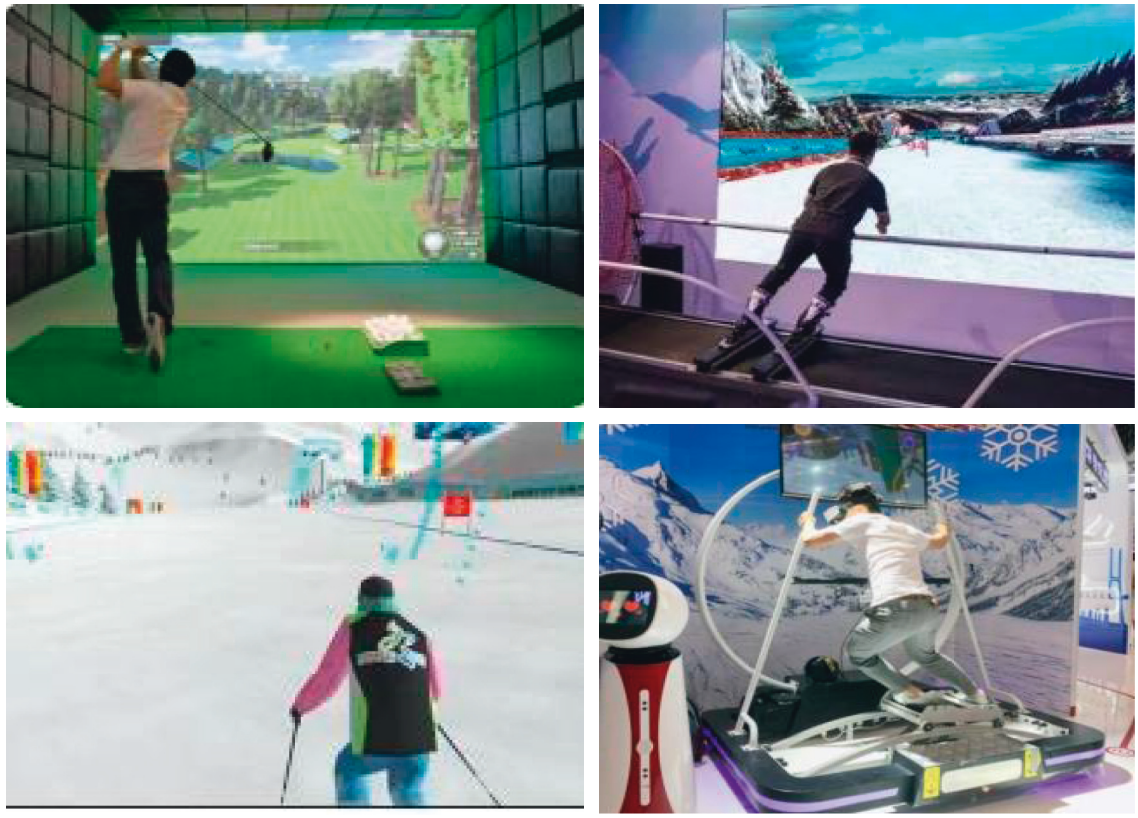

Figure 1: The fusion of modern sports and mobile information technology.

2.2. Dilemma of Cross-Country Skiing. Cross-country skiers are usually in the process of high-speed movement when they make mistakes, so the accident damage caused by mistakes is irreversible. Identifying cross-country skiing mistakes is an important step in danger warning. The analysis of the dangerous state in the process of cross-country skiing can effectively and accurately realize the triggering measures of danger warning for cross-country skiers [15]. The common fall postures during skiing are shown in Figure 2.

As shown in Figure 2, the center of gravity of the skier is out of balance, the body leans back, and the back is on the ground. The skier's center of gravity moves forward and lies on his stomach, with the chest, head, and elbow as the key injured parts. Comprehensive skiing ubiquitous and cross-country skiing specific dangerous conditions can be seen: the change of sports trends is an important factor in the occurrence of dangerous conditions in cross-country skiing.

2.3. Gesture Recognition Algorithm

2.3.1. Complementary Filtering Algorithm. The essence of the complementary filtering attitude fusion method is to eliminate the noise between the data for data fusion, which is a typical frequency domain filtering method. When using multiple sensors to detect the target signal, the detection signal has some noise in the frequency domain, and the frequency bands of the noise of different sensors will be different. The influence of noise on the results can effectively improve the detection advantage of the sensor [16].

Fixed-gain complementary filter (FGCF) is used for joint 3D attitude estimation of two or more types of inertial sensors (IMUs). When using a single IMU for attitude calculation, the data noise of the inertial sensor itself has a great influence on the calculation result [17].

First, use the valid data on the accelerometer and gyroscope sides to calculate the cross product of the gravitational acceleration measured by the accelerometer and the theoretical gravitational acceleration. The vector cross product of the accelerometer data is used to measure the error of the sensor data. The cross product formula is

$$|\vec{C}| = |\vec{V}| + |\vec{g}| \sin\theta. \tag{1}$$

The vector is unitized, because the error of the measurement data of the correct use of the sensor in practical applications will not be too large, so it can be deduced:

$$|\vec{C}| = \sin\theta \approx \theta = Er. \tag{2}$$

With the help of the PID (proportional, integral, differential) feedback control idea, the PI controller is used to control the compensation value of the skier's gyroscope data and set the appropriate proportional gain and integral gain value. In general, Kp is 10–100 times larger than Ki, and Ki may be as low as 0.002. The PI controller is as follows:

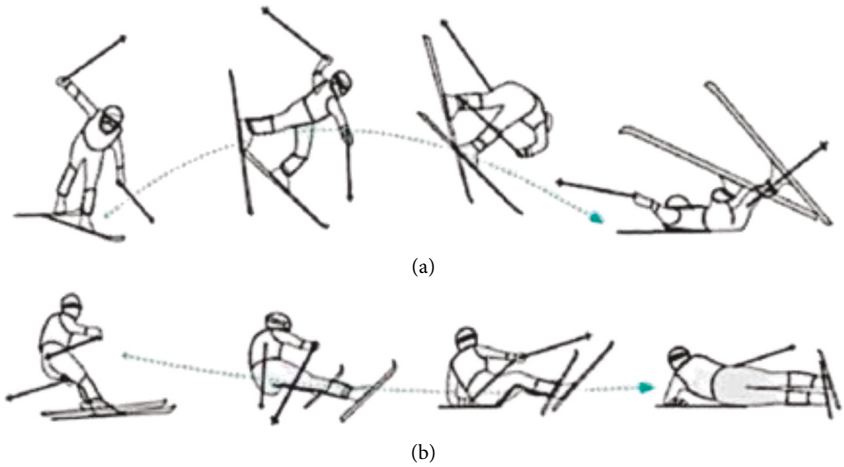

(a)

(b)

Figure 2: Typical fall posture during cross-country skiing. (a) Skier is projected into the air. (b) Skier skips and rolls.

$$Er_{\mathrm{GYRO}} = H_c * Er + H_l \int Er. \tag{3}$$

The proportional term is used to control the reliability of the sensor, and the compensation value calculated by the PI controller is added to the angular velocity to obtain gyroscope data with high reliability. Solve, according to the updated attitude data to obtain the effective skier attitude angle [18].

$$\mathrm{Re\_GYRO} = \mathrm{Re\_GYRO} + Er\_\mathrm{GYRO}. \tag{4}$$

2.3.2. Modeling and Analysis of Attitude Calculation System. After the attitude measurement system completes the data acquisition task of the target movement process, it calculates the attitude data according to the actual needs. The calculation can be completed independently by a single inertial sensor and can be combined with multiple types of sensors to perform data fusion according to the characteristics of the inertial sensor detection data. In this method the premise is to be able to master the characteristics and methods of attitude calculation of a single sensor [19].

(1) Model Design of Gyroscope Attitude Calculation. Gyroscopes have high sensitivity to the detection of angular changes of target motion and are widely used in aircraft, inertial navigation, wearable smart equipment, and other fields [20]. Since the gyroscope mainly detects the angular rate of the target based on the coordinate axis transformation, the data form is displayed as the three-axis angular rate of x, y, and z, but the obtained value cannot directly display the real angle value, and the corresponding coordinate transformation and other related calculations need to be established. The solution model between the gyroscope output data and the attitude angle:

$$\begin{aligned}
\overset{a}{\omega}_{ia} &= \overset{a}{\omega}_{ie} + \overset{a}{\omega}_{en} + \overset{a}{\omega}_{na},\\
\overset{a}{\omega}_{na} &= \overset{a}{\omega}_{ia} - \begin{pmatrix} \overset{a}{\omega}_{ie} + \overset{a}{\omega}_{en} \end{pmatrix},\\
\overset{a}{\omega}_{na} &= \overset{a}{\omega}_{ia} - C_n^a \begin{pmatrix} \overset{a}{\omega}_{ie} + \overset{a}{\omega}_{en} \end{pmatrix}.
\end{aligned} \tag{5}$$

The actual output of the gyroscope is set as $\overset{a}{\omega}_{ia}$, $\overset{a}{\omega}_{ia}$ is projected $\overset{a}{\omega}_{ie}$ in the carrier coordinate system (b system) by the Earth's rotation, and the rotation angle of the base coordinate system (n system) relative to the Earth is transformed to project ω_{en}^a and the carrier coordinate system in the carrier coordinate system. The movement angle transformation value $\overset{a}{\omega}_{na}$ relative to the base coordinate system is composed of three parts, and $\overset{a}{\omega}_{na}$ is the reference data of the attitude angle calculated by the gyroscope.

The base coordinate system is used as the fixed coordinate system, and the carrier coordinate system is used as the reference coordinate system. The Euler angles of the angular transformation of the movement of the carrier coordinate system relative to the base coordinate system are determined as pitch angle θ, roll angle Y, and heading angle ψ. Then it can be deduced that the relationship between $\overset{a}{\omega}_{na}$ and attitude Euler angle is as follows:

$$\begin{bmatrix} \overset{a}{\omega}_{\mathrm{nax}} \\ \overset{a}{\omega}_{\mathrm{nay}} \\ \overset{a}{\omega}_{\mathrm{naz}} \end{bmatrix} = A_\gamma A_\theta \begin{bmatrix} 0 \\ 0 \\ -\psi \end{bmatrix} + A_\gamma \begin{bmatrix} \theta \\ 0 \\ 0 \end{bmatrix} + \begin{bmatrix} 0 \\ \gamma \\ 0 \end{bmatrix} = \begin{bmatrix} \cos\gamma & 0 & \sin\gamma\cos\theta \\ 0 & 1 & -\sin\theta \\ \sin\gamma & 0 & -\cos\theta\cos\gamma \end{bmatrix} \begin{bmatrix} \theta \\ \gamma \\ \psi \end{bmatrix}. \tag{6}$$

Among them, when the set value of the gyroscope sampling period is small, the relationship between $\overset{a}{\omega}_{na}$ and attitude Euler angle can be simplified as follows:

$$\begin{bmatrix} a \\ \omega \\ \text{nax} \\ a \\ \omega \\ \text{nay} \\ a \\ \omega \\ \text{naz} \end{bmatrix} = \begin{bmatrix} a \\ \omega \\ \text{iax} \\ a \\ \omega \\ \text{iay} \\ a \\ \omega \\ \text{iaz} \end{bmatrix} = \begin{bmatrix} \cos\gamma & 0 & \sin\gamma \\ \sin\gamma & 1 & -\sin\gamma \\ \sin\gamma/\cos\theta & 0 & -\cos\gamma/\cos\theta \end{bmatrix} \begin{bmatrix} \theta \\ \gamma \\ \psi \end{bmatrix}. \tag{7}$$

Quaternion is introduced to solve the related attitude. The quaternion solution attitude calculation relationship is as follows:

$$\overset{\rightarrow}{\overset{e}{E}} = \frac{1}{2}\Omega_b\left(\omega_{na}^a\right)\overset{e}{E}. \tag{8}$$

Among them, $\Omega_b\left(\omega_{na}^a\right)$ is the angular velocity motion vector of the gyroscope output target motion, and its matrix form is as follows:

$$\begin{bmatrix} \overset{\rightarrow}{0} \\ e \\ \overset{\rightarrow}{1} \\ e \\ \overset{\rightarrow}{2} \\ e \\ \overset{\rightarrow}{3} \\ e \end{bmatrix} = \frac{1}{2} \begin{bmatrix} & a & a & a \\ 0 & \omega & \omega & \omega \\ & \text{nax} & \text{nay} & \text{naz} \\ a & & a & a \\ \omega & 0 & \omega & \omega \\ \text{nax} & & \text{naz} & \text{nay} \\ a & a & & a \\ \omega & \omega & 0 & \omega \\ \text{nay} & \text{naz} & & \text{nax} \\ a & a & a & \\ \omega & \omega & \omega & 0 \\ \text{naz} & \text{nay} & \text{nax} & \end{bmatrix} \begin{bmatrix} 0 \\ e \\ 1 \\ e \\ 2 \\ e \\ 3 \\ e \end{bmatrix}. \tag{9}$$

Set the sampling period of the gyroscope as T, and within the sampling period T, the $\Omega_b\left(\omega_{na}^a\right)$ direction remains unchanged. Using the Picard approximation method to solve the target motion matrix, we can get

$$E_e(t+T) = e^{0.5\int_t^{t+T}\Omega_b\left(\omega_{na}^a\right)\mathrm{d}t},$$

$$[\Delta\theta] = \int_t^{t+T}\Omega_b\left(\omega_{na}^a\right)\mathrm{d}t = \begin{bmatrix} 0 & \Delta\theta_x & \Delta\theta_y & \Delta\theta_z \\ \Delta\theta_x & 0 & \Delta\theta_z & \Delta\theta_y \\ \Delta\theta_y & \Delta\theta_z & 0 & \Delta\theta_x \\ \Delta\theta_z & \Delta\theta_y & \Delta\theta_x & 0 \end{bmatrix}. \tag{10}$$

Solving the above two formulas together, we get

$$E_e(t+T) = E_e(t)e^{0.5[\Delta\theta]} = E_e(t)\left\{\cos\frac{\Delta\theta_0}{2}I + \frac{\sin/}{\Delta\theta_0}[\Delta\theta]\right\}. \tag{11}$$

Using the quaternion to solve the gyroscope to measure the attitude angle, the result is

$$\begin{cases} \theta = \arcsin\left[2\left(e_2e_3 + e_0e_1\right)\right], \\ \gamma = \arctan\left[-\dfrac{2\left(e_1e_3 - e_0e_2\right)}{e_0^2 - e_1^2 - e_2^2 + e_3^2}\right], \\ \psi = \arctan\left[\dfrac{2\left(e_1e_3 - e_0e_2\right)}{e_0^2 - e_1^2 - e_2^2 + e_3^2}\right]. \end{cases} \tag{12}$$

(2) Design of Accelerometer Attitude Calculation Model. The accelerometer measures the motion acceleration relative to the base coordinate system during the movement of the target and is widely used in various fields such as intelligent sports equipment, motion planning, and motion control [21]. In practical applications, the actual output measurement value of the accelerometer belongs to the specific force, including the effect of all forces detected by the accelerometer during the target movement, so the accelerometer cannot be directly used as the acceleration value of the target space movement. The actual output specific force equation of the accelerometer is as follows:

$$f_{ia}^a = g_{ea}^a + \left(2\omega_{ie}^e + \omega_{ea}^a\right) \times g_{ea}^a + g_a. \tag{13}$$

Among them, f_{ia}^a is the actual output value of the accelerometer, that is, the measured value of the specific force; $\overset{a}{g}_{ea}$ represents the motion acceleration of the carrier coordinate system relative to the Earth coordinate system; $\left(2\omega_{ie}^e + \omega_{ea}^a\right) \times g_{ea}^a$ represents the sum of the Coriolis acceleration and the normal acceleration of the target motion measured by the accelerometer; $\overset{a}{g}$ the target gravitational acceleration is measured for the accelerometer [22].

When the target motion is in a stationary state or a uniform motion state, it can be known that the motion

acceleration of the target is 0, ignoring the Coriolis acceleration and the normal acceleration during the target motion, namely, $(2\omega_{ie}^{e} + \omega_{ea}^{a}) \times g_{ea}^{a} = 0$; then the accelerometer actually measures the gravitational acceleration of the target motion, it can be deduced that

$$\begin{bmatrix} f_{iax}^{a} \\ f_{iay}^{a} \\ f_{iaz}^{a} \end{bmatrix} = \begin{matrix} a \\ C \\ n \end{matrix} \begin{bmatrix} 0 \\ 0 \\ g \end{bmatrix} = -g \begin{bmatrix} \sin\gamma\cos\theta \\ \sin\theta \\ \cos\gamma\cos\theta \end{bmatrix}. \tag{14}$$

The attitude angle model can be calculated by the accelerometer from the above formula. Due to the data detection characteristics of the accelerometer, the accelerometer can only solve the pitch angle θ_{acc} and roll angle γ_{acc} of the target motion. The specific calculation process is as follows:

$$\begin{cases} \theta_{acc} = \arcsin\left(-\dfrac{f_{iay}^{a}}{g}\right), \\ \gamma_{acc} = \arcsin\left(-\dfrac{f_{iax}^{a}}{g\cos\theta_{acc}}\right). \end{cases} \tag{15}$$

3. Experiment and Analysis of Human Posture Recognition in Cross-Country Skiing Resistance Training System

Corresponding principles should be followed when designing a skier's attitude recognition system. It is necessary to ensure the timely, stable, and reliable performance of the system. The most important thing is the accuracy of system recognition. Therefore, these performances should be guaranteed in the process of hardware and software design of the system. First of all, when the system collects human body posture, it needs quick response to collect human body data and remove environmental errors, because human body movement is irregular, fast, and affected by surrounding environmental factors; secondly, in the design process, hardware equipment also needs to consider its sensitivity, to be able to collect human motion data in a timely manner; then, when the system is put into use, its cost is a factor that must be considered, in the selection of components not only to ensure the effect, but also to reduce its cost; finally, in order to make the system application convenient and fast, it is required to achieve a high degree of integration in the system design process, so that the user can achieve the goal with simple operation. After the system design is completed, each part of the system can achieve the expected purpose, and the following functions can be realized on the whole.

(1) Acquisition function. The sensor is worn on the main joint points of the human body, and the network camera placed in the training scene is used to collect human motion data, which provides a data basis for the system to recognize the human body posture.

(2) Transmission function. The data information of human motion is sent in two ways: the sensor part is sent wirelessly through ZigBee, and the network camera is sent through Ethernet. The underlying network is networked through the ZigBee coordinator to form a specific network for data transmission, and finally the collected data is sent to the host computer through the ESP8266 wireless module connected to the coordinator. The two parts of the system send data to the host computer in different ways.

(3) Data processing function. Since the data of the sensor on the Z-axis is prone to drift, Kalman filtering is used to process the data after the data is collected, and the data is processed and sent to the upper computer to drive the motion of the human body model.

(4) Interface display function. The human body model is built by modeling software, and the exported FBX file is imported into Unity3D. When the system starts to run, the data collected by sensors and webcams will drive the human body model to move.

(5) Teaching function. During the training process of skiers, the system will collect a large amount of human motion information, which improves the real-time analysis, and can provide timely result analysis and data feedback during training. Through this visual method, coaches can clearly point out the deficiencies of the athletes in the existing technical level and give timely guidance and propose a series of targeted improvement plans, thereby improving the teaching level. Athletes can also build their own sports information database and conduct targeted training, get rid of the original way of groping in repetitive training, and greatly improve training efficiency.

3.1. Architecture of Human Gesture Recognition System

3.1.1. Overall Design Scheme of Human Gesture Recognition System. The human body gesture recognition system is composed of three parts: sensor acquisition unit, network camera part, and host computer. This paper firstly carries out the overall planning according to the requirements of the system; secondly, the experimental test is carried out to test whether it is reasonable. Then, the hardware design scheme of the acquisition module and camera in the system is proposed, and the hardware equipment is selected according to the scheme; finally, the software that can complete the system tasks is selected and programmed to complete the overall design scheme. The overall design of the system is shown in Figure 3.

As shown in Figure 3, this paper designs 11 acquisition modules, which are worn near the main joints of the human body. The built-in inertial sensor MPU9150 chip and CC2530 chip are used to read the data of the internal registers of the sensor and process the data to obtain the key

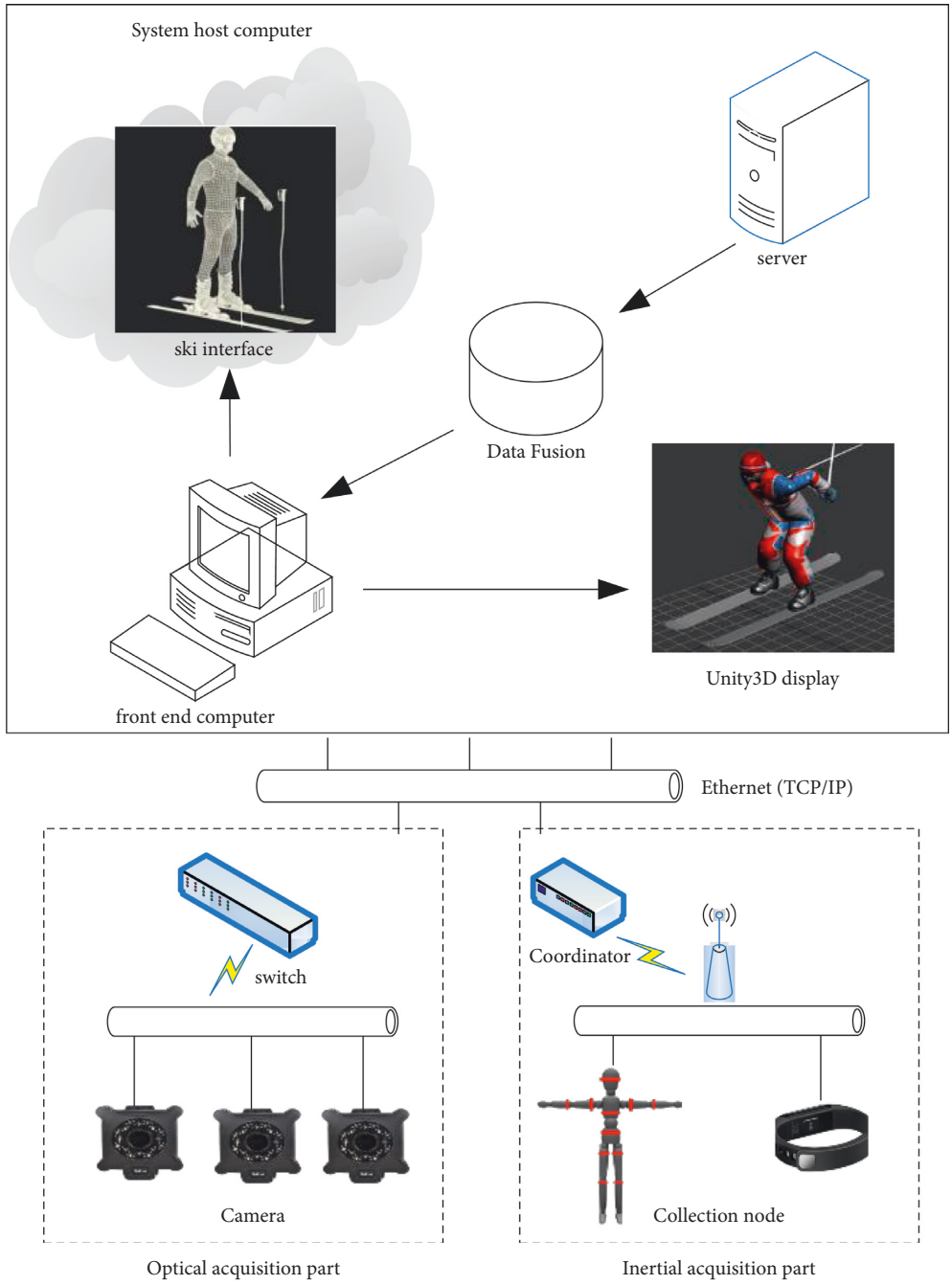

Figure 3: Overall design of the system.

points of human movement. The data information of the node: the camera part uses the network camera to act as the human eye and sticks the Marker point of the reflective material on the human body. The two-dimensional coordinates of the Marker point can be determined through two cameras, and its three-dimensional coordinates can be determined through multiple cameras. The actual three-dimensional coordinates of the human body are calculated by the three-dimensional coordinates of the Marker point, so as to infer the actual posture of the human body; the coordinates of the Marker point collected and calculated by the network camera and the joint attitude data obtained by the acquisition unit are subjected to big data fusion analysis to obtain accurate attitude data. The upper computer part first uses modeling software to build a human body model and then imports the established human body model into Unity3D and receives the fusion processing data of the lower computer in Unity3D, thereby driving the movement of the human body model and providing a visual interface display. People can intuitively see the changes of the posture and posture data of the human body during the movement process in the interface.

3.1.2. Inertial Acquisition Design Framework. The acquisition unit mainly includes acquisition sensor, processing unit module, communication unit module, and host computer display unit. The acquisition sensor in the system uses the 9-axis MPU9150 module; the processing unit uses the CC2530 chip; the transmission method is wireless based on the ZigBee network and uses a mesh-type network topology; finally, the host computer uses Unity3D for animation simulation. First, the acquisition module is worn on the main joint points of the human body, and the joint data information of human motion is collected through the MPU9150 inertial sensor, and the measured analog quantity will be converted into three 16-bit digital quantities that can be output. And the human body posture is described in the form of quaternion or Euler angle. Due to the instability of the Z-axis and the accompanying offset characteristics at the initial stage of power-on of the module, the system is required to measure 3 minutes after power-on. The Kalman filtering method is used to complete the calculation of the data. The module sends data to the host computer, and finally the Script (script) drives the human body model in Unity3D, so as to visualize the motion and posture of the human body. The system diagram of the acquisition unit is shown in Figure 4.

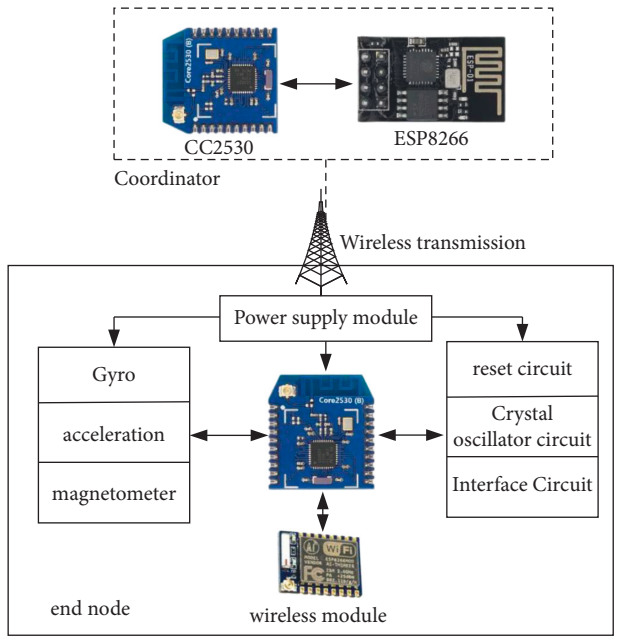

Figure 4: System diagram of acquisition unit.

As shown in Figure 4, the ZigBee terminal node worn on the human body uses the protocol stack provided by TI. The network part is composed of the ZigBee coordinator and ESP8266, which is the first device to start in the entire system. It is used for networking, and then the terminal nodes are added to the network. Each terminal node has its own ID number, which is used to distinguish sensors in different locations. The ZigBee coordinator is connected to the ESP8266 wireless module, so that the data in the entire network can be sent to the host computer.

3.1.3. Fusion in Time. In this system, the fusion in time mainly refers to synchronizing the data of the inertial sensor MPU9150 with the data of the camera in time, so that the data collected by the system when capturing human motion information is the information of human motion at the same time. However, in general, the sampling frequencies of sensors and cameras are different, and each sensor and camera cannot interfere with each other during operation. Therefore, when collecting data, there will be a data information problem that the data collected by the sensor and the camera are not at the same time. Temporal information fusion is shown in Figure 5.

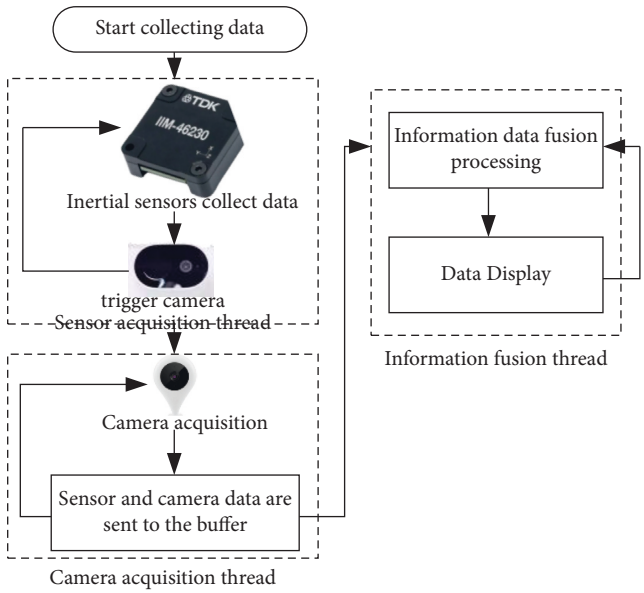

Figure 5: Information fusion over time.

As shown in Figure 5, the operating frequency of the inertial sensor MPU9150 used in the system is 20 Hz, and the operating frequency of the camera is significantly greater than that of the sensor. Therefore, the system uses multithreading to process sensor data, camera data, and data fusion, respectively, so that the collected data can be synchronized in time. Because the frequency of the camera is higher than the frequency of the sensor, the sensor data is always accepted first when collecting data. When the data collection thread of the sensor returns the information, the camera immediately collects the data information at the current moment and transmits it to the fusion thread; turn off the camera again. In the system, this process has been repeated so that the collected data can be synchronized in time. Finally, it is combined with spatial data fusion to complete the system to collect the attitude information of skiers.

3.2. Experimental Analysis of High-Intensity Resistance Training System for Cross-Country Skiing. During the nearly 6-month-long land training in the preparation period, according to the training plan, according to the needs of

Table 1: Statistics of morphological indicators of cross-country skiers before and after training.

	Gender	Height (cm)	Weight (kg)	Calf	Thigh	Body fat (%)
Pretraining	Male	176.9 ± 3.68	70.2 ± 1.63	37.6 ± 0.71	56.1 ± 1.20	14.2 ± 0.51
	Female	165.4 ± 3.99	56.3 ± 2.02	35.1 ± 0.53	51.8 ± 1.41	18.4 ± 0.48
Posttraining	Male	176.9 ± 3.68	70.1 ± 1.20	37.8 ± 0.83	56.9 ± 0.97	14.2 ± 0.37
	Female	165.4 ± 3.99	56.7 ± 1.92	35.5 ± 0.43	52.3 ± 1.43	18.2 ± 0.48

cross-country skiers' upper and lower limbs, waist, and abdominal muscles and other special endurance training needs, a combination of high-strength training and special endurance training was adopted. In addition to the specific cardiopulmonary function of athletes, the morphological parameters of athletes can reach or be close to the "ideal" body morphological parameters of elite cross-country skiers.

In the small-cycle plan for special endurance training in the preparatory period, we have arranged the strengthening training of the upper and lower limbs and waist and abdominal muscles of the athletes in a targeted manner. During the whole training period, each athlete will perform endurance training 6–9 times a week, each time about 1 to 4 hours or about 15–90 minutes of strength training. The endurance training plan for athletes in the preparatory period was as follows: in the first three months, endurance training accounted for 66% and strength training accounted for 34%; in the last three months, endurance training accounted for 58% and strength training accounted for 42%. Routine endurance training includes cross-country pulley, cross-country running, imitation training with sticks, etc. The high-strength training includes explosive training, jumping in different ways, and cross-country pulley sprinting exercises, such as triple jump, sixth-level jump, ten-level jump, and short distance jumping. The second is resistance training, which is a combination of special training forms such as barbell squats with 70%–90% RM and weight-bearing pulley sliding. After the training, the male and female athletes were tested for morphological indicators, physiological and biochemical indicators of cardiopulmonary function, special endurance quality, and cross-country pulley performance.

3.2.1. Comparison of Morphological Indicators. Before the training period, the athletes' body shape indicators were measured. The average height of men is about 176.9 cm, the average weight is about 70.2 kg, the circumference of the thigh is about 56.1 cm, the circumference of the calf is about 37.6 cm, and the circumference of the upper arm is about 31.6 cm. The average body fat percentage is about 14.2%: the average height of women is about 1654 cm, the average weight is about 56.3 kg, the thigh circumference is about 51.8 cm, the average calf circumference is about 35.1 cm, the average upper arm circumference is about 29.9 cm, and the average body fat percentage is about 18.4%; they were measured after training in the land period. The statistics of morphological indicators of cross-country skiers before and after training are shown in Table 1.

As shown in Table 1, the average height of men is about 176.9 cm, the average weight is about 70 kg, the average thigh circumference is about 56.9 cm, the average calf circumference is about 37.8 cm, the average upper arm circumference is about 32.3 cm, and the average body fat percentage is about 14%. The average height of women is about 165.4 cm, the average weight is about 56.7 kg, the thigh circumference is about 523 cm, the calf circumference is about 35.5 cm, the upper arm circumference is about 30.6 cm, and the body fat percentage is about 18.2%. By comparison, it was found that the thigh circumference of both men and women increased slightly, the weight of women, calf circumference, and upper arm circumference increased slightly, and the percentage of body fat decreased slightly for both men and women. Table 2 shows the paired t-test of the morphological index data of athletes before and after training in the preparatory period.

As shown in Table 2, Figure 2 shows the changes in body size metrics for cross-country skiers. The weight of male athletes decreased slightly, but there was no significant difference compared with the pretraining test, while the percentage of body fat decreased, and the circumference of the calf and thigh increased. There is an increase, about 0.4 kg, and there is a significant difference. At the same time, the percentage of body fat decreases, $p < 0.05$, and the circumference of the calf and the thigh both slightly increase. These changes reflect that this stage of training reduces the fat content of the athletes, increases the muscle volume of the upper and lower limbs, and thus increases the lean body mass. Both men and women show the muscular characteristics of excellent cross-country skiers.

3.2.2. Comparison of Physiological Indicators. The statistics of the physiological indicators of athletes before and after training in the preparatory period and the land period are shown in Table 3.

It can be seen from Table 3 that, after the training in the athlete's preparation period, the average resting heart rate of the eight male athletes is about 58.37 beats/min, which is about 0.25 beats/min lower than that before training, 2.37 beats/min; heart rate increased by about 2.5 beats/min after training; absolute VO2 max increased by about 0.11 on average; relative VO2 increased by about 1.63 ml; VO2 max plateau increased on average about 21.5 seconds; the anaerobic threshold increased by about 1.39% on average. The seven female athletes decreased by about 1 beat/min after training; the peak heart rate was increased by about 2.86 beats/min after training; the heart rate was increased by about 3.57 beats/min after training; absolute VO2 max average increased by about 0.19; the relative maximum

Table 2: Paired t-test for the data of athletes' morphological indicators before and after training in the preparatory period.

	Index	Mean	Std. deviation	Std. error	Lower	Upper	t
Male	Weight	0.20000	1.93686	0.68478	−1.41926	1.81926	0.292
	Calf	−0.18750	0.30909	0.10928	−0.44590	0.07090	−1.716
	Thigh	−0.48750	0.41897	0.14813	−0.83777	−0.13723	−3.291
	Body fat percentage	0.23750	0.26152	0.09246	0.01886	0.45614	2.569
Female	Weight	−0.41429	0.25448	0.09619	−0.64964	−0.17893	4.307
	Calf	−0.37143	0.33523	0.12671	−0.68147	−0.06139	−2.931
	Thigh	−0.44286	0.35989	0.13603	−0.77570	−0.11001	−3.256
	Body fat percentage	0.24286	0.15119	0.05714	0.10303	0.38268	4.250

Table 3: Statistics of physiological indicators of athletes before and after training in the preparatory period.

	HR	HR_{max}	HRR	VO_{2max}		VO_{2max}PD
	Beat/min	Beat/min	Beat/min	$L{\cdot}min^{-1}$	$ml{\cdot}kg^{-1}{\cdot}min^{-1}$	sec
Pre	58.62 ± 1.92	188.75 ± 2.60	130.12 ± 3.31	5.09 ± 0.18	72.76 ± 1.68	151.12 ± 18.49
	59.71 ± 2.21	186.71 ± 3.30	127.28 ± 3.49	3.36 ± 0.13	59.87 ± 0.78	138.14 ± 19.91
Post	58.37 ± 2.06	191.12 ± 2.85	132 62 ± 3.99	5.20 ± 0.14	74.39 ± 1.99	172.62 ± 19.54
	58.71 ± 1.88	189.57 ± 2.57	130.85 ± 4.18	3.55 ± 0.14	63.01 ± 1.15	156.85 ± 19.43

oxygen uptake increased on average by about 3.14 ml; the maximum oxygen uptake plateau increased on average by about 18.71 seconds; the anaerobic threshold increased by about 1.67% on average. Table 4 shows the paired t-test of the data on the physiological indicators of athletes before and after training in the preparatory and land periods.

Table 4 shows the statistics and paired t-test of some physiological index data obtained from the two exercise treadmill experiments before and after the land training in the preparatory period. Combining the two tables, it can be seen that there is no major change in men's and women's basic heart rate before and after training, but the peak heart rate (HRmx) and heart rate reserve (HRR) after extreme load have increased, and the paired t-test $p < 0.05$, showing significance difference. The size of the heart rate reserve reflects the adaptability of the heart pumping function to the metabolic demands. Athletes can promote the thickening of myocardial fibers through training, increase coronary blood flow, improve myocardial contractility, increase heart rate reserve, and thus improve cardiac reserve. For example, when an athlete is exercising vigorously, the heart rate can reach 2 to 3 times the resting time, so the myocardial contractility is greatly improved, and the ejection rate and relaxation rate are significantly accelerated, which not only increases the cardiac output but also promotes the rapid return of venous blood to the heart, thereby increasing the duration of high-intensity exercise in athletes.

3.2.3. Comparison of Special Endurance Quality Indicators. After the training in the preparatory period, the special endurance quality of the athletes was tested. At present, when the training team is training in the snow-free period, the special endurance of the upper limbs is generally trained by imitating the cross-country skiing double-arm support technique, mainly using the method of pulling rubber bands. The special strength endurance of the lower limbs mainly uses the resistance training method; the strength and endurance training of the waist and abdominal muscles is often carried out with weight-bearing sit-ups, two-head ups, etc. By soliciting the suggestions of experts and coaches, three items were selected from the special endurance training items often used by athletes for testing. The maximum number of times of pulling the rubber band with the arms simulating cross-country skiing in 3 minutes, 2 kg for men and 1.5 kg for women, is used to evaluate the effect of upper body strength and endurance; the maximum number of times of lifting from both heads in 3 minutes is used to evaluate the effect of abdominal muscle strength and endurance; the maximum number of repetitions of weight-bearing barbell squatting, 60 kg for men and 50 kg for women, is used to evaluate the effect of lower body strength and endurance. Figure 6 shows the comparison of the special endurance quality performance test of cross-country skiers in the preparatory period and the Lu period.

As shown in Figure 6, it can be seen that the strength and endurance of the upper limbs have been greatly improved before and after training for both men and women. The maximum number of rubber band pulling in 3 minutes increased by 22.5 times on average for men and about 23.6 times for women. The p-values of paired t-test before and after training were 0.000 and 10.001, respectively, with a very significant difference; abdominal muscle endurance was also greatly improved, especially for men; women improved about 20.9 times on average; the paired t-test p-values before and after training were 0.008 and 0.162, respectively; there was a significant difference in men, and $p > 0.5$ in women had no significant difference, indicating that women's abdominal muscle training effect is relatively poor, possibly because the training intensity is not enough, suggesting that the training of abdominal muscle endurance should be

Table 4: Paired t-test of the data on the physiological indicators of athletes before and after training in the preparatory period.

	Index	Mean	Std. deviation	Std. error	Lower	Upper	t
Male	HR	0.250	1.03	0 365	−0.615	1.115	0.683
	HR_{max}	−2.375	1.18	0.419	−3.367	−1.382	−5.656
	HRR	−2.500	1.60	0.566	−3.840	−1.159	4.410
	$VO_{2\,max}$	−0.1125	0.079	0.028	−0.178	−0.046	4.016
Female	HR	1.00	0.377	0.377	0.0751	1.924	2.646
	HR_{max}	−2.857	0.799	0.799	−4.813	−0.900	−3.573
	HRR	−3.571	0.782	0.782	−5.486	−1.656	−4.564
	$VO_{2\,max}$	0.194	0.023	0.023	0.2512	−0.137	−8.344

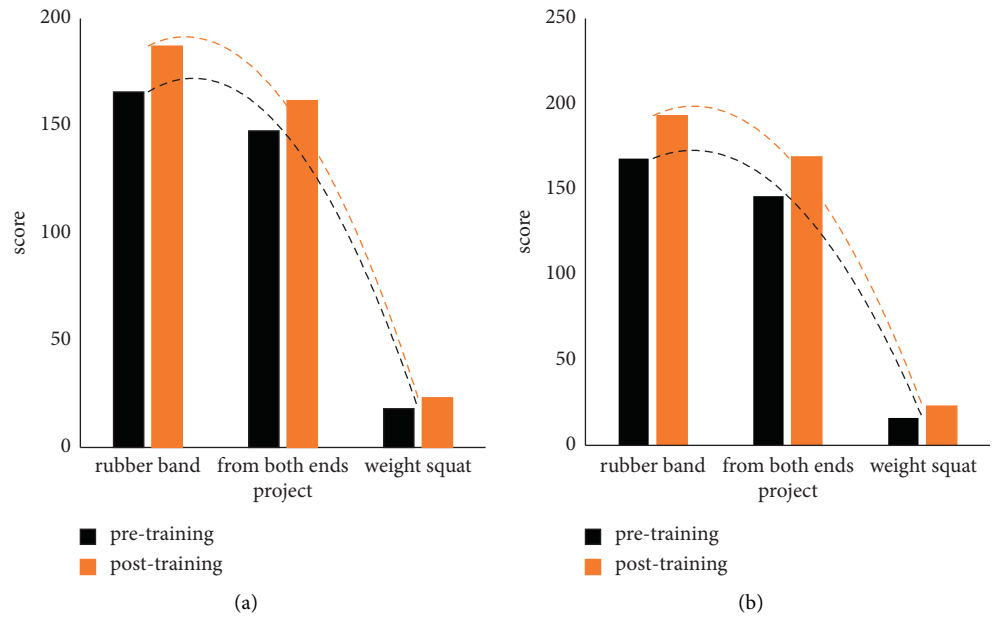

Figure 6: Comparison of the special endurance quality performance test of cross-country skiers in the preparatory period and the Lu period. (a) Before and after training for men. (b) Before and after training for women.

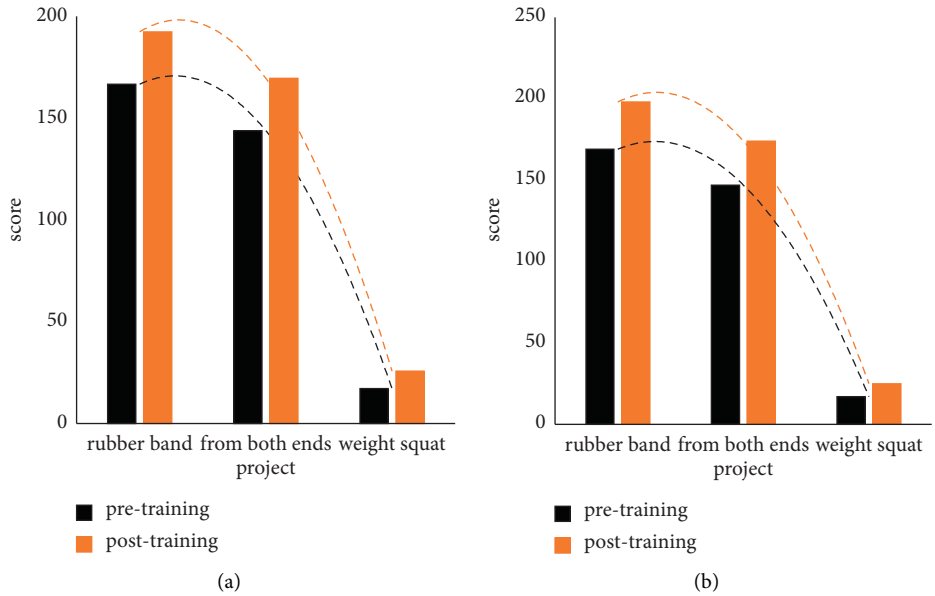

Figure 7: Comparison of athletes' specific endurance quality performance test after snow training and before land training in the preparation period. (a) Before and after training for men. (b) Before and after training for women.

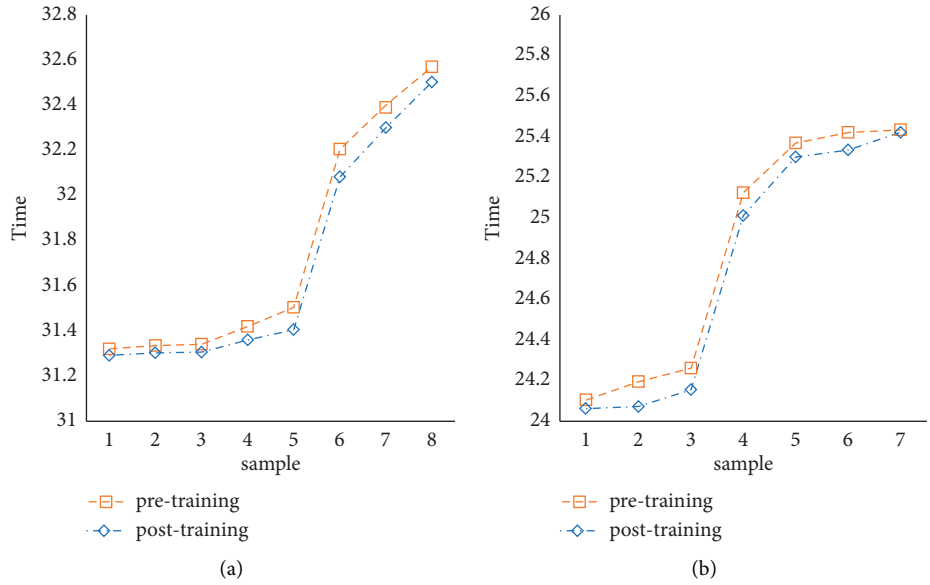

Figure 8: Comparison of performance tests of cross-country skiers before and after land training during the preparation period. (a) Before and after training for men. (b) Before and after training for women.

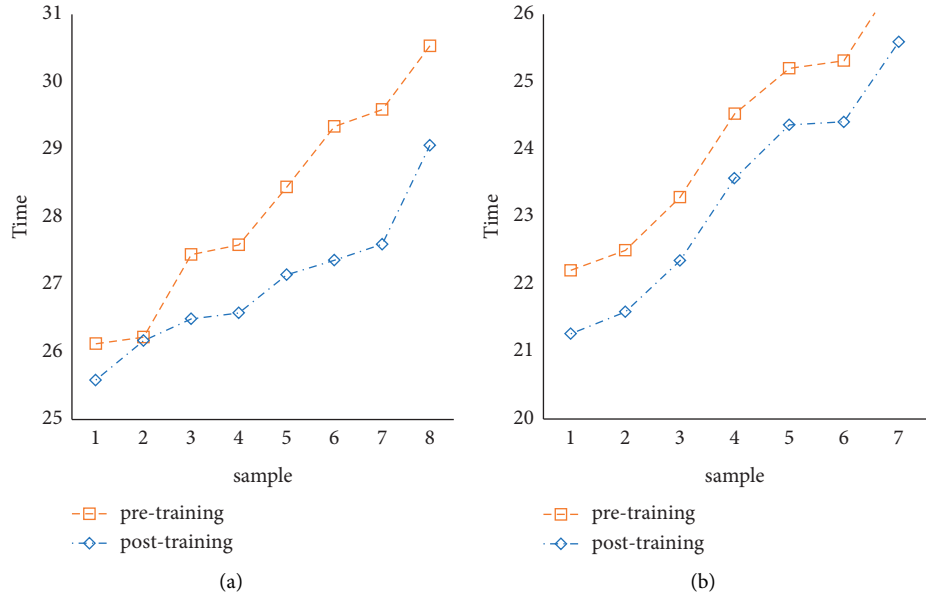

Figure 9: Statistics on the comparison of performance tests before and after snow training for cross-country skiers during the preparation period. (a) Before and after training for men. (b) Before and after training for women.

strengthened in the future training; the lower limb endurance has improved significantly, in particular the female lower limb strength endurance has improved greatly, the women increased by an average of 5.2 times, and the paired t-test p-values were 0.01 1 and 0.003 before and after training, suggesting a significant difference. Figure 7 shows the comparison of athletes' specific endurance quality performance test after snow training and before land training in the preparation period.

As shown in Figure 7, it is a comparison histogram of the specific endurance quality data measured by athletes after the snow training and before the land training. It can be seen from the figure that the specific endurance qualities of athletes after training in snow-capped mountains are improved to varying degrees regardless of whether male or female athletes are trained on land. The comprehensive analysis of each index reflects that the athletes' muscular endurance quality has been greatly improved in the

preparatory training stage, and it also reflects the rationality and effectiveness of the special endurance quality training methods and means in this stage.

3.2.4. Comparison of Cross-Country Skiing Performance. The comparison of the specific endurance qualities of male and female athletes before and after training shows that the specific endurance of the upper limbs is relatively improved, indicating that the effect of training on the upper limbs is more obvious at this stage, which also reflects the training characteristics of cross-country skiing that focus on the strength and endurance of the upper limbs. Figure 8 shows the comparison of the performance test of cross-country skiers before and after land training in the preparation period.

As shown in Figure 8, the pretest and posttest are in the same training field, and the cross-country pulleys and canes used by the athletes are the same pair. All use traditional skiing techniques. The fastest time for men was $31'\ 29''\ 21$, which was $1''\ 88$ higher than before training, and the average score improved $6''\ 80$; the fastest time for women was $24'\ 06''\ 21$, which was $4''\ 22$ higher than before training, and the average score was improved $7''\ 70$. Figure 9 shows a comparison of the two field cross-country skiing performance tests before and after the snow training in the preparation period.

As shown in Figure 9, after the athletes entered the snow training in the preparatory period, they conducted two cross-country skiing tests. The first time we switched from land to snow training for about a week. After we started to adapt to snow training, we took a performance test as a pretest indicator for longitudinal comparison. The second test was conducted after training on the snow. The men's test was a traditional 10 km cross-country skiing event and the women's traditional 7.5 km.

4. Conclusions

In recent years, with the success of China's bid to host the Winter Olympics, sports on ice and snow have attracted more and more attention, and people have become more and more keen on ice and snow sports. Starting from the systematicness, scientific implementation, and real-time nature of training structure, this research is based on system theory, cybernetics, information theory, and dissipative structure theory and is refined through questionnaires, expert interviews, and the rich training experience of front-line coaches. Based on the training results, a special endurance annual training plan is formulated based on the training structure, but the current human posture recognition technology is mainly used in large-scale sports, such as basketball, gymnastics, and other projects, system research, and design. In the previous human gesture recognition system, a single sensor or camera is mainly used to collect human body data and perform gesture capture. The use of sensors for acquisition has the problem of low acquisition accuracy, which cannot meet the needs of skiing. Using an optical camera to collect human body data will easily block body parts due to bending, kneeling, and other actions during the skiing process, resulting in inaccurate data collection. In this context, a human gesture recognition system that effectively combines sensors and optical cameras can make up for the above shortcomings.

Data Availability

No data were used to support this study.

Conflicts of Interest

The authors declare that they have no conflicts of interest.

Acknowledgments

This paper was supported by Business Expense Project of Fundamental Scientific Research of Undergraduate Universities within Heilongjiang Province (2021KYYWF-FC15).

References

[1] P. T. Reidy, M. S. Borack, M. M. Markofski et al., "Post-absorptive muscle protein turnover affects resistance training hypertrophy," *European Journal of Applied Physiology*, vol. 117, no. 5, pp. 853–866, 2017.

[2] V. Freitas, "Monitoring of the internal training load in futsal players over a season," *Journal of Clinical Investigation*, vol. 91, no. 5, pp. 2020–2030, 2017.

[3] B. C. Miller, A. W. Tirko, J. M. Shipe, O. R. Sumeriski, and K. Moran, "The systemic effects of blood flow restriction training: a systematic review," *International Journal of Sports Physical Therapy*, vol. 16, no. 4, pp. 978–990, 2021.

[4] M. Drummond, L. A. Szmuchrowski, and R. Simo, "Effect of local vibration during resistance exercise on muscle hypertrophy," *Journal of Exercise Physiology Online*, vol. 20, no. 5, pp. 69–79, 2017.

[5] D. Maleev, A. Isaev, J. Petrova, V. Zalyapin, A. Shevtsov, and Y. Korableva, "Statokinetic and hypoxia resistance," *Human Sport Medicine*, vol. 20, no. 1, pp. 43–51, 2020.

[6] R. Dias, R. J. Baganha, F. Cieslak et al., "Parâmetros imunol ó gicosinfec çõesdotratorespiratóriosuperiorematle tasdeesportescoletivos," *Revista Brasileira de Medicina do Esporte*, vol. 23, no. 1, pp. 66–72, 2017.

[7] L. Zhu, "Computer vision-driven evaluation system for assisted decision-making in sports training," *Wireless Communications and Mobile Computing*, vol. 2021, no. 7, pp. 1–7, 2021.

[8] R. Babu and D. Heath, "Mobile assistive technology and the job fit of blind workers," *Journal of Information, Communication and Ethics in Society*, vol. 15, no. 2, pp. 110–124, 2017.

[9] V. Rosso, V. Linnamo, W. Rapp et al., "Simulated skiing as a measurement tool for performance in cross-country sit-skiing," *Proceedings of the Institution of Mechanical Engineers - Part P: Journal of Sports Engineering and Technology*, vol. 233, no. 4, pp. 455–466, 2019.

[10] N. Kurpiers, P. Mcalpine, and U. G. Kersting, "A biomechanical field testing approach in snow sports: c," *Proceedings of the Institution of Mechanical Engineers - Part P: Journal of Sports Engineering and Technology*, vol. 234, no. 4, pp. 337–346, 2020.

[11] V. Bittner, R. Štryncl, K. Jelen, and M. Svoboda, "Mathematical model of the RRR anthropomorphic mechanism for 2D biomechanical analysis of a deep squat and related forms of movement," *Manufacturing Technology*, vol. 18, no. 5, pp. 704–708, 2018.

[12] Y. Sun, R. Guo, L. Gao, C. Wu, and H. Zhang, "Research on the inrun profile optimization of ski jumping based on dynamics," *Structural and Multidisciplinary Optimization*, vol. 63, no. 3, pp. 1481–1490, 2021.

[13] C. Yuanxiang, J. Haiyan, and F. Jianqiang, "Research on sports dance teaching and training practice simulation based on virtual environment," *Boletin Tecnico/Technical Bulletin*, vol. 55, no. 20, pp. 283–288, 2017.

[14] J. M. Cholewa, A. Hewins, S. Gallo et al., "The effects of moderate- versus high-load resistance training on muscle growth, body composition, and performance in collegiate women," *The Journal of Strength & Conditioning Research*, vol. 32, no. 6, pp. 1511–1524, 2018.

[15] B. M. Da, S. Rachael, S. Selvaraj, C. A. Greig, R. M. Aspden, and T. Frank, "Sex differences in the effect of fish oil supplementation on the adaptive response to resistance exercise training in older people: a randomized control trial[J]," *The American Journal of Clinical Nutrition*, vol. 105, no. 1, pp. 151–158, 2017.

[16] M. Wilk, A. Golas, P. Stastny, M. Nawrocka, M. Krzysztofik, and A. Zajac, "Does tempo of resistance exercise impact training volume?[J]," *Journal of Human Kinetics*, vol. 62, no. 1, pp. 241–250, 2018.

[17] J. Chen, Z. Lv, and H. Song, "Design of personnel big data management system based on blockchain," *Future Generation Computer Systems*, vol. 101, pp. 1122–1129, 2019.

[18] H. Zhu, H. Wei, B. Li, X. Yuan, and N. Kehtarnavaz, "Real-time moving object detection in high-resolution video sensing," *Sensors*, vol. 20, no. 12, p. 3591, 2020.

[19] J. K. Ihalainen, J. P. Ahtiainen, S. Walker et al., "Resistance training status modifies inflammatory response to explosive and hypertrophic resistance exercise bouts," *Journal of Physiology & Biochemistry*, vol. 73, no. 4, pp. 595–604, 2017.

[20] N. V. O. Bento-Torres, J. Bento-Torres, A. M. Tomas et al., "WATER-BASED exercise and resistance training improve cognition in older adults," *Revista Brasileira de Medicina do Esporte*, vol. 25, no. 1, pp. 71–75, 2019.

[21] R. Bertuzzi, A. F. Gaspari, L. R. Trojbicz et al., "Commentaries on Viewpoint: resistance training and exercise tolerance during high-intensity exercise: moving beyond just running economy and muscle strength," *Journal of Applied Physiology*, vol. 124, no. 2, pp. 529–535, 2018.

[22] S. Tomiya, N. Kikuchi, and K. Nakazato, *Journal of Sports Science and Medicine*, vol. 16, no. 3, pp. 391–395, 2017.